Volume 5 | Number 4 | July 2018 | Pages 581–754

# Materials Horizons

rsc.li/materials-horizons

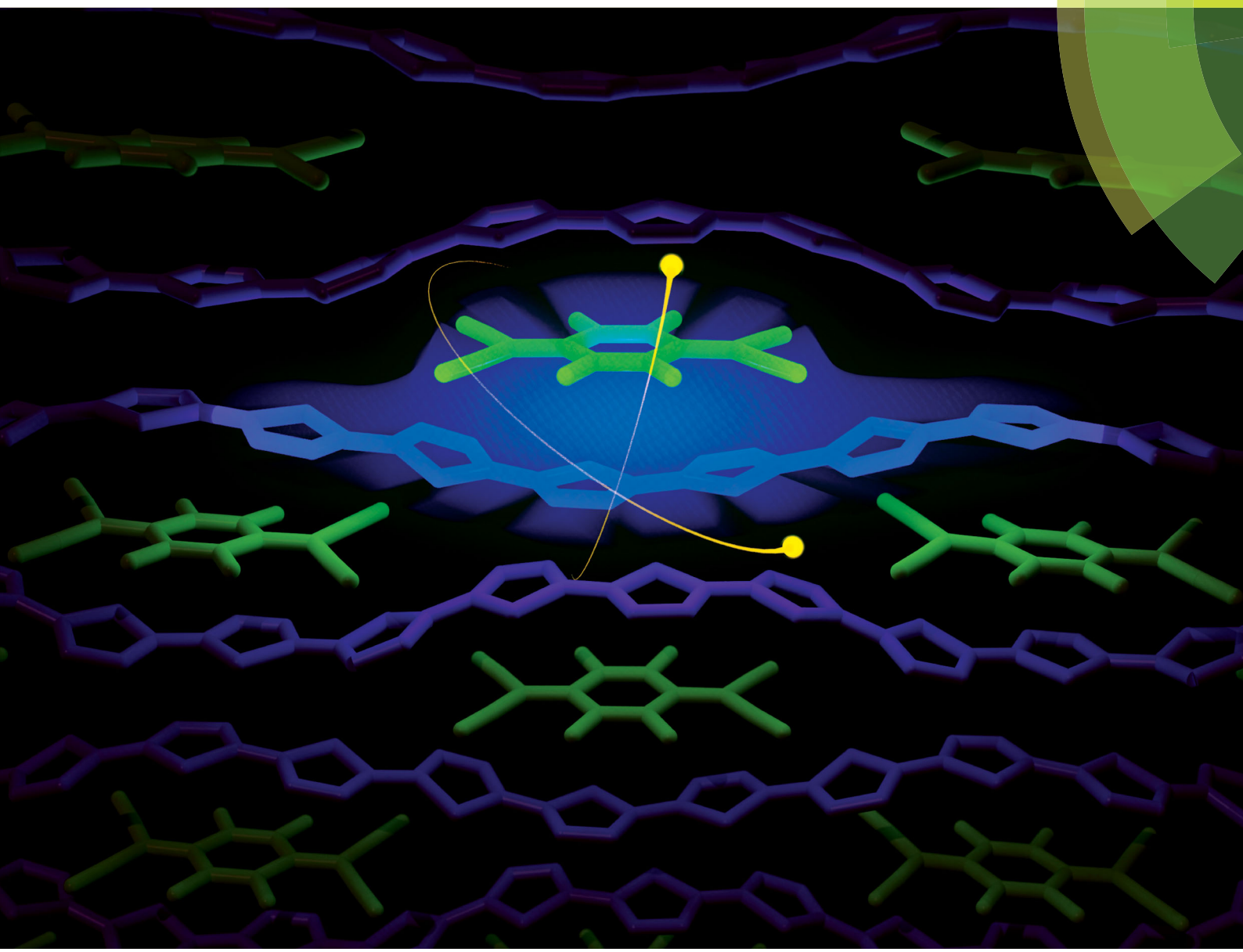

ISSN 2051-6347

ROYAL SOCIETY OF CHEMISTRY

COMMUNICATION

Adam J. Moulé *et al.*

Polymorphism controls the degree of charge transfer in a molecularly doped semiconducting polymer

Materials Horizons

COMMUNICATION

View Article Online
View Journal | View Issue



Cite this: *Mater. Horiz.*, 2018, 5, 655

Received 20th February 2018,
Accepted 26th March 2018

DOI: 10.1039/c8mh00223a

rsc.li/materials-horizons



# Polymorphism controls the degree of charge transfer in a molecularly doped semiconducting polymer†

Ian E. Jacobs, ‡[a] Camila Cendra,[b] Thomas F. Harrelson, [c] Zaira I. Bedolla Valdez,[c] Roland Faller, [c] Alberto Salleo[b] and Adam J. Moulé *[c]

**When an organic semiconductor (OSC) is blended with an electron acceptor molecule that can act as a p-type dopant, there should ideally be complete (integer) transfer of charge from the OSC to the dopant. However, some dopant–OSC blends instead form charge transfer complexes (CTCs), characterized by fractional charge transfer (CT) and strong orbital hybridization between the two molecules. Fractional CT doping does not efficiently generate free charge carriers, but it is unclear what conditions lead to incomplete charge transfer. Here we show that by modifying film processing conditions in the semiconductor–dopant couple poly(3-hexylthiophene):2,3,5,6-tetrafluoro-7,7,8,8,-tetracyanoquinodimethane (P3HT:F4TCNQ), we can selectively obtain nearly pure integer or fractional CT phases. Fractional CT films show electrical conductivities approximately 2 orders of magnitude lower than corresponding integer CT films, and remarkably different optical absorption spectra. Grazing incidence wide-angle X-ray diffraction (GIXD) reveals that fractional CT films display an unusually dense and well-ordered crystal structure. These films show lower paracrystallinity and shorter lamellar and π-stacking distances than undoped films processed under similar conditions. Using plane-wave DFT we obtain a structure with unit cell parameters closely matching those observed by GIXD. This first-ever observation of both fractional and integer CT in a single OSC–dopant system demonstrates the importance of structural effects on OSC doping and opens the door to further studies.**

### Conceptual insights

Doping is a fundamental tool in semiconductor engineering, yet is still poorly understood in organic semiconductors (OSCs). Two different doping mechanisms have been observed in OSCs—integer charge transfer and fractional charge transfer—corresponding to the amount of charge exchanged between the OSC and each dopant molecule. All OSC:dopant systems studied to date exclusively display either fractional or integer CT, regardless of doping level or processing conditions. Puzzlingly, structurally similar OSCs (*e.g.* polythiophenes *vs.* thiophene oligomers) sometimes dope by different mechanisms.[1] Although intramolecular hybridization between the dopant and OSC molecular orbitals should be an important factor, it is currently impossible to predict which mechanism will be active in a given OSC:dopant system. Here we observe for the first time both fractional and integer CT in a single OSC:dopant system. Both phases exist as well-ordered crystalline polymorphs, can be fabricated at identical doping levels at high purity, and can be interconverted by solvent exposure. In addition to providing a much needed model system for future comparative studies, these results suggest that molecular structure (*i.e.* intermolecular hybridization) alone does not determine the degree of charge transfer, and that ionic lattice packing (Madelung energy), charge delocalization, and/or dimerization could conceivably play equally important roles.

Over the past decade, breakthroughs in the theoretical understanding of molecularly doped organic semiconductors[1,2] and control of doped film morphology[3] have reinvigorated research interest in doped organic semiconductors (OSCs). Doping is a crucially important process in the design and fabrication of electronic devices. Doped OSCs find applications as active layers in organic thermoelectrics,[4] as carrier-selective transport layers in organic light emitting diodes and photovoltaics,[5] and in several areas of organic thin-film transistors.[6] Unfortunately, doping most OSCs is non-trivial; many OSCs are unaffected by molecular dopants, even with favorable energy-level alignment. This behavior is poorly understood and limits device applications.

One significant issue, identified by the Koch group in a string of recent papers,[1,7–10] is that two distinct doping mechanisms exist. In systems displaying relatively efficient doping, such as the semiconducting polymer poly(3-hexylthiophene) (P3HT) blended with the p-type molecular dopant 2,3,5,6-tetrafluoro-7,7,8,8,-tetracyanoquinodimethane (F4TCNQ), doping results in ion pair (IP) formation. This mechanism is characterized by integer charge transfer (CT) from the polymer to the dopant molecule and little hybridization between the molecular orbitals

[a] *Department of Materials Science and Engineering, University of California, Davis, USA*
[b] *Department of Materials Science and Engineering, Stanford University, Stanford, USA*
[c] *Department of Chemical Engineering, University of California, Davis, USA. E-mail: amoule@ucdavis.edu*

† Electronic supplementary information (ESI) available. See DOI: 10.1039/c8mh00223a

‡ Present address: Cavendish Laboratory, University of Cambridge, Cambridge, UK.

(MOs) of the OSC and dopant. However, in the structurally similar oligomer quaterthiophene, doping with F4TCNQ produces charge transfer complexes (CTCs), characterized by fractional charge transfer to the dopant and strong hybridization between the OSC and dopant MOs.[1,3,9] CTCs must thermally dissociate into free charge carriers,[1,7] and therefore show lower carrier density and electrical conductivity than systems that dope by IP formation.[9,10]

Currently, it is not possible to predict whether CTC or IP formation will occur in a given OSC:dopant system. It is also unclear why CTC formation is not a general phenomenon, given that DFT simulations predict strong orbital coupling between OSC and dopant.[11,12] Previous work suggests that IP *vs.* CTC formation might be controlled by dopant strength.[1] However, charge localization, *e.g.* on the donor subunit of donor–acceptor polymers,[10,13,14] or on small molecule OSCs[7–9] may also encourage CTC formation. Increased disorder upon doping, as observed in pentacene:F4TCNQ, could also play a role.[7,15] However, our understanding of what controls CTC formation has been hampered by the fact that experimentally, a given OSC always forms either CTCs or IPs, regardless of dopant molecule or concentration.[1–3]

In this communication, we describe a P3HT:F4TCNQ crystalline polymorph which gives rise to CTC formation, but can be subsequently converted to the standard IP polymorph by solvent exposure. This is the first observation of selective CTC or IP formation in a single OSC:dopant system. P3HT:F4TCNQ is already a model system in the study of doping; we expect studies of this unexpected fractional CT polymorph to help refine our understanding of doping interactions.

Fig. 1a shows UV-vis-NIR spectra of several P3HT films doped with 13 mol% F4TCNQ prepared using the mixed-solution method, in which the P3HT and F4TCNQ solutions are mixed before spin-coating.[16] Doping strongly reduces the solubility of P3HT,[17] therefore mixed P3HT:F4TCNQ solutions are generally suspensions[16] and must be processed at low concentrations and elevated temperatures to prevent large-scale aggregation or gelling.[16,18–21] Although this is the primary method used to prepare P3HT:F4TCNQ films in the literature, we were nonetheless surprised to discover that if the P3HT:F4TCNQ mixed solution is kept solvated throughout the coating process by heating the solution, pipette tips, and substrates to 80 °C, the resulting films bear little resemblance to those previously reported.

A spectrum of one of these films is shown in blue in Fig. 1a. This film clearly lacks spectral signatures from either F4TCNQ, $F4TCNQ^{\bullet-}$, or P3HT and cannot be generated by a linear combination of neutral and ionized species, strongly suggesting that orbital hybridization (*i.e.* CTC formation) is occurring. At first glance, the strong absorption band at 2.0 eV might appear to be a red-shifted absorption band of neutral P3HT. However, this is not the case. Almost no neutral F4TCNQ is present in these samples, as confirmed by the FTIR spectrum in Fig. 1b. This observation, along with past studies showing 17 mol% F4TCNQ doping fully bleaches the P3HT π–π* band,[16,18,22] indicates that little neutral P3HT remains in the film. The absorption features

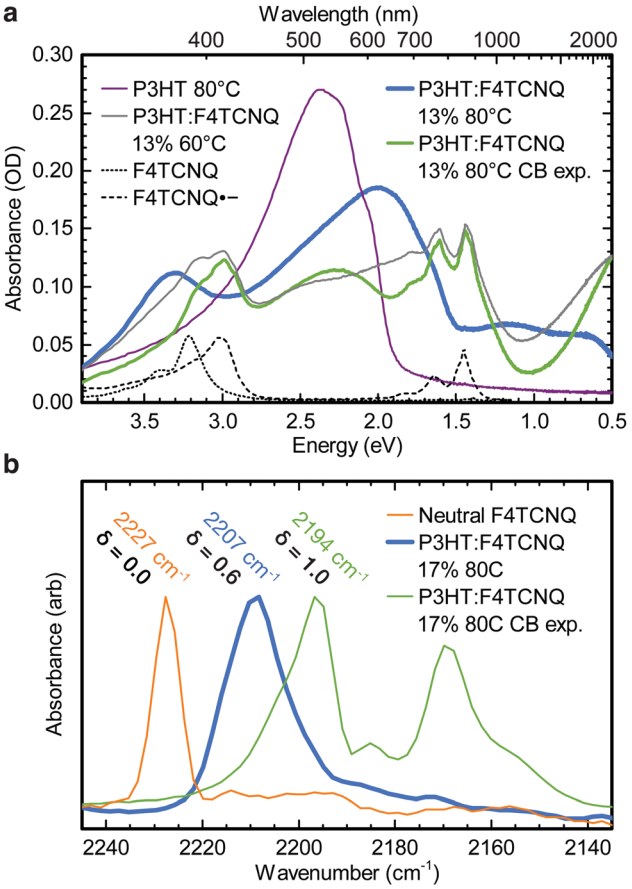


Fig. 1 (a) UV-vis-NIR of P3HT:F4TCNQ 13 mol% thin films spin-coated from mixed solution using pre-heated substrates and glass pipettes. Spectra of an undoped P3HT film and acetonitrile solutions of F4TCNQ and $F4TCNQ^{\bullet-}$ are shown for reference. Film samples are between 35 and 38 nm thick. (b) Detail of thin-film FT-IR spectra showing the –CN stretch region of F4TCNQ. Peak position and calculated degree of charge transfer (δ) is shown above.

at ~1 eV, 2.0 eV, and 3.4 eV are also broadly consistent with those predicted by DFT simulations of thiophene oligmer:F4TCNQ complexes.[23] Therefore, the spectrum shown here in blue instead appears to result from a P3HT:F4TCNQ CTC.

We can rule out the possibility of a chemical reaction, such as thermal decomposition of F4TCNQ, because exposure to chlorobenzene (CB) converts the film to the normally observed state (green line). Note that P3HT:F4TCNQ films are insoluble in CB above ~3 mol% F4TCNQ loading.[17] The CB exposed spectrum is similar to an as-cast film processed at a lower temperature (60 °C, gray line) and previous reported spectra of P3HT:F4TCNQ.[9,16–18,21,22,24,25]

Tetracyanoquinodimethanes (TCNQs) undergo a softening of the –CN stretch vibrational band upon ionization.[9,11,26] In neutral F4TCNQ this band appears at 2227 $cm^{-1}$ (Fig. 1b, orange line), and undergoes a linear shift to 2194 $cm^{-1}$ as the degree of charge transfer (δ) goes to 1.[26] Therefore, Fourier transform infrared (FTIR) spectroscopy is often used to experimentally measure δ and to determine whether doping is occurring *via* CTC or IP formation.[1,3,9] In P3HT:F4TCNQ 17 mol% processed

 

at 80 °C (Fig. 1b, blue line), the –CN stretch occurs at 2207 $cm^{-1}$, corresponding to $\delta$ = 0.6. This observation confirms that CTC formation is occurring in the 80 °C film. After CB exposure, the –CN stretch shifts to 2194 $cm^{-1}$. This matches previously reported spectra for P3HT:F4TCNQ, indicating integer CT and IP formation.[9]

The fractional CT phase seen in the 80 °C processed films is very sensitive to film casting conditions. We are only able to reliably obtain the nearly pure fractional CT films shown in Fig. 1 using low molecular weight P3HT (25 kDa) and compositions between 13 mol% and 17 mol% F4TCNQ. Atomic force microscopy of the fractional CT films (ESI,† Section S3) reveals significantly more phase separation at 17 mol% than 13 mol%, suggesting that the CTC phase has a well-defined stoichiometry near 13 mol% F4TCNQ. Film processing details are provided in the ESI.†

Electrical conductivity measurements are shown in Table 1. As expected for CTC mediated doping, the fractional CT films show lower conductivity than typically observed in integer CT films.[16,18,22,27] After CB exposure to convert the films to the integer CT phase, the conductivities increase 2 orders of magnitude to values consistent with previous reports.[16,18,22,27] However, since the pure CTC phase should behave as an undoped material,[9] it is unclear whether the fractional CT phase conductivity values represent the intrinsic conductivity of the phase, or are affected by neutral polymer/dopant impurities. The somewhat higher conductivity observed in the 13 mol% fractional CT sample may also be due to residual integer CT phase impurities, which become visible in UV-vis-NIR spectra at lower doping levels (see ESI,† Section S3) and would dominate the measurement if present due to their higher conductivity.

To characterize the film microstructure giving rise to this unusual doped phase, we collected grazing-incidence wide-angle X-ray diffraction (GIXD) patterns of thin films prepared identically to those shown in Fig. 1a. All films were between 35 and 38 nm thick and coated from similar solution concentrations at identical spinning speed to minimize the role of film processing conditions on microstructure. Shortly after coating, the films were cooled to −78 °C to prevent further microstructural evolution during transport. Therefore, the differences in the 2D-GIXD images shown in Fig. 2 should primarily result from interactions between the polymer and dopant during coating.

The GIXD data in Fig. 2a reveal that the fractional CT films are composed of a new crystalline polymorph distinct from both undoped P3HT (Fig. 2d) and integer CT P3HT:F4TCNQ (Fig. 2c). Both the lamellar (100) and π–π (010) stacking distances of the fractional CT phase are significantly smaller

Table 1 In-plane conductivity (S $cm^{-1}$) for P3HT:F4TCNQ films doped at 13 mol% and 17 mol%

| | 13 mol% | 17 mol% |
|---|---|---|
| 80 °C as cast (Fractional CT) | $4.2 \times 10^{-2}$ $\pm 9 \times 10^{-3}$ | $1.6 \times 10^{-2}$ $\pm 2 \times 10^{-3}$ |
| 80 °C CB exp. (Integer CT) | 2.1 $\pm 8 \times 10^{-2}$ | 3.2 $\pm 2.4 \times 10^{-1}$ |

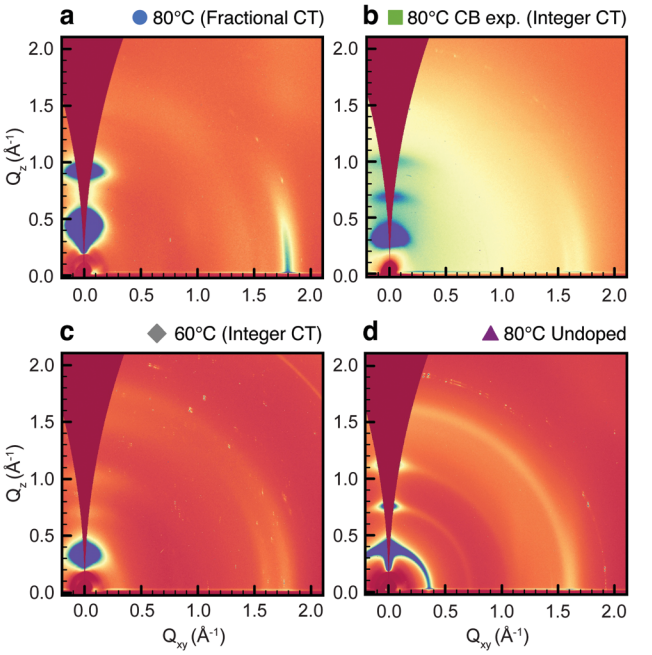


Fig. 2 Grazing-incidence X-ray diffraction (GIXD) patterns for P3HT:F4TCNQ 13 mol% thin films prepared identically to those shown in Fig. 1a.

than in undoped P3HT or integer CT phase P3HT:F4TCNQ, as shown in Fig. 3a. Previously studied (integer CT) P3HT:F4TCNQ films showed an increase in the lamellar (100) spacing, along with a splitting of the π-stacking (010) peak, consistent with the 60 °C and 80 °C CB exposed films shown in Fig. 2b and c.[9,18,19]

We also observe increased crystalline order in the fractional CT films. As shown in Fig. 3b, the fractional CT phase shows a longer π–π (010) coherence length and lower paracrystallinity than the other samples, including undoped P3HT. Additionally, the fractional CT films show stronger edge-on texture than other films. These effects likely result from favorable ionic interactions in the π-stacking direction. Raman spectroscopy (ESI,† Section S7) corroborates these findings. Previous Raman studies have shown

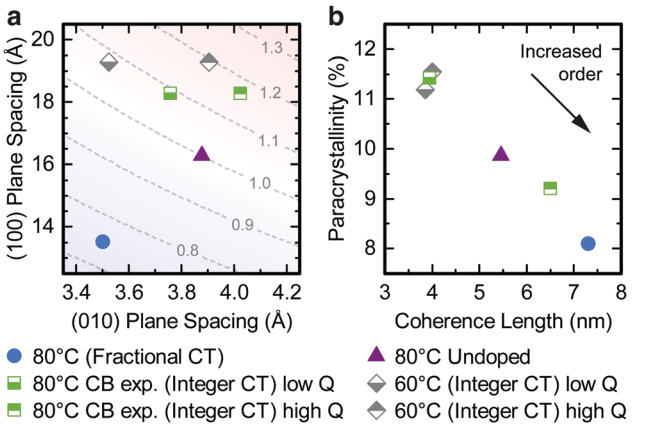


Fig. 3 (a) (100) and (010) plane spacings obtained from GIXD data in Fig. 2. Dotted lines indicates unit cell volume relative to undoped P3HT. (b) Coherence length and paracrystallinity in the π-stacking [010] direction, obtained from data in Fig. 2.

a red-shift of the C=C peak in integer CT P3HT:F4TCNQ, which was assigned to polymer backbone planarization.[12,28–30] We observe a similar red-shift in the fractional CT phase, indicating a comparable increase in backbone planarity.

The increased order in the fractional CT phase relative to the integer CT phase indicates that in this system, fractional charge transfer does not originate from disorder-induced charge localization.[28,29] Therefore, some change in the crystal structure must be directly affecting the degree of charge transfer.

To better understand the atomic-scale structure of these polymorphs, we performed plane-wave DFT structural minimizations for several candidate crystal structures (see ESI,† Section S8) corresponding to both the integer and fractional CT phases. Fig. 4 shows a structure obtained from an unconstrained plane-wave DFT simulation that is remarkably consistent with the experimental unit cell dimensions obtained from GIXD (Table 2). In this structure, the short lamellar stacking distance is possible due to a shift in the stacking order of adjacent lamella, creating an "interlocked" side chain arrangement in which the dopant molecule is flanked by side chains from adjacent polymers. This was the only structure which showed lamellar stacking distances consistent with the fractional CT GIXD results. Therefore, it seems likely that the fractional CT phase adopts this type of interlocked packing motif.

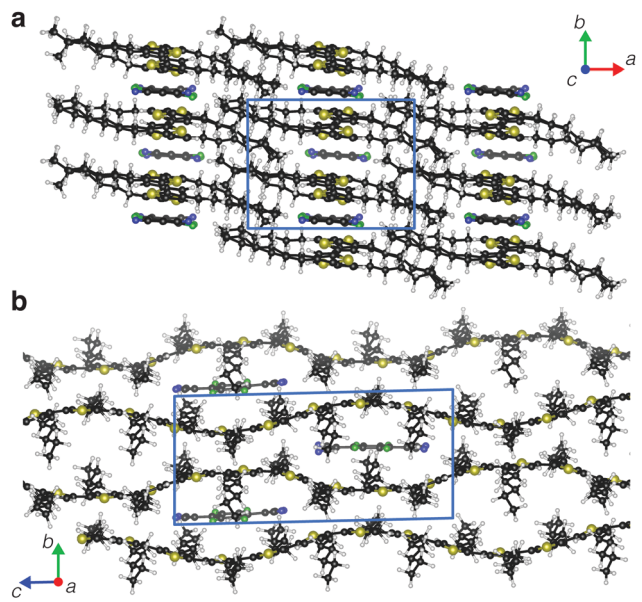


Fig. 4 Plane-wave DFT structure corresponding to the fractional CT phase, viewed (a) parallel to the polymer chains, and (b) parallel to the lamellar stacking direction. The simulation contains 6 P3HT monomers per F4TCNQ molecule, equivalent to 14.2 mol% doping.

Table 2 Unit cell parameters for the fractional CT phase obtained from GIXD and DFT

| Direction | GIXD (Å) | DFT (Å) |
|---|---|---|
| *a* [100] (lamellar) | 13.57 | 13.58 |
| *b* [010] (π–π) | 3.48 | 3.51 |

DFT has not been shown to quantitatively predict the degree of charge transfer,[11] likely due to a combination of charge localization errors[31] and small unit cell sizes which inadequately capture long-range structure.[32] These issues are compounded in plane-wave DFT, where periodic boundary conditions results in valence orbital delocalization over the entire material.[33] All structures we simulated showed fractional CT ($\delta < 0.6$); detailed results are given in ESI,† Section S8.

Given the limitations of DFT, we intentionally limit our analysis of these results. However, some insights about charge distribution can be gained from the literature of organic charge transfer salts, which share many similarities with doped OSCs.[34] Pressure-dependent neutral-ionic phase transitions have been observed in CT salts, where an increase in the Coulombic interaction between the hole/dopant and the surrounding ionic lattice (called the Madelung energy) as the unit cell is compressed causes an increase in CT.[35] Counterintuitively, we observe the opposite dependence in our system—denser packing in P3HT:F4TCNQ leads to a decrease in CT.

Theoretical models of these systems predict that a reduction in either the Madelung energy or the CTC transfer integral could decrease the degree of CT.[36,37] Both of these factors could result from changes in hole delocalization on the polymer, which is not considered in these theories. However, charge localization in the fractional CT phase doesn't appear to adequately explain our results. Increased order in the fractional phase, as seen in GIXD (Fig. 3) and Raman (ESI,† Section S7), should instead prompt more charge delocalization and a greater degree of CT. Alternatively a reduction in Madelung energy, driven by repulsive interactions along the shortened lamellar stacking direction, could conceivably give fractional CT. However, due to the aforementioned delocalization concerns we do not attempt such a calculation here.

We observe one last feature in our DFT structures worth noting. In the structure shown in Fig. 4, the F4TCNQ molecules seem to be interacting with both adjacent P3HT chains (*i.e.* non-dimerized), while in other proposed integer CT structures (Fig. S13 and S14, ESI† and previous work by Harrelson *et al.*[38]) each F4TCNQ molecule is associated primarily with a single P3HT chain (*i.e.* dimerized). It is possible that interactions from both adjacent F4TCNQ molecules may be acting to localize charges on the polymer, increasing the transfer integral. Dimerization effects of this type have been routinely observed in the context of charge transfer salts, where dimerization or Peierls transitions often occur alongside neutral–ionic transitions.[35,36,39–41] Interestingly, one of these models[36] identifies a region which is non-dimerized but remains ionic. This region corresponds to an area in which charge transfer is exothermic ($HOMO_D < LUMO_A$, as in P3HT:F4TCNQ) but the Madelung energy is small. The degree of charge transfer in this region is less than 1, but an increase in Madelung energy should result in a system with nearly integer CT and a dimerized lattice, consistent with our results.[36] However, we note that this model neglects the coupling between donor units (as would be the case for a p-type doped polymer), and considers only nearest neighbor ionic interactions. Theoretical models of these systems show a range of

 

complex behavior.[36,37,42,43] Further experimental, computational, and theoretical work will be necessary to understand the precise role crystal structure plays in doping interactions.

Incomplete charge transfer is a major barrier to efficient doping in OSCs, but the factors controlling charge transfer are poorly understood. We have identified a polymorph of the well studied P3HT:F4TCNQ system that displays fractional charge transfer, but reverts to the typically observed integer CT phase upon exposure to solvent. This is the first OSC:dopant system which selectively displays both fractional and integer CT, and opens the door to further experimental and computational studies on the role crystal structure plays in controlling doping efficiency.

## Conflicts of interest

There are no conflicts to declare.

## Acknowledgements

This work was funded by the National Science Foundation Scalable Nanomanufacturing Program, Award # CMMI 1636385. IEJ thanks the Department of Energy, BES Award No. DE-SC0010419 for additional funding. CC and AS acknowledge financial support from the National Science Foundation, Award # CMMI 1636385 and CBET 1510481 respectively. ZIBV acknowledges the SENER-CONACyT program for funding. Part of this work was performed at the Stanford Nano Shared Facilities (SNSF), supported by the National Science Foundation under award ECCS-1542152. GIXD measurements were carried out at the Stanford Synchrotron Radiation Lightsource, a national user facility operated by Stanford University on behalf of the U.S. Department of Energy, Office of Basic Energy Sciences. We also gratefully acknowledge NERSC for computational time.



## References

1 I. Salzmann, G. Heimel, M. Oehzelt, S. Winkler and N. Koch, *Acc. Chem. Res.*, 2016, **49**, 370–378.
2 I. Salzmann and G. Heimel, *J. Electron Spectrosc. Relat. Phenom.*, 2015, **204**, 208–222.
3 I. E. Jacobs and A. J. Moulé, *Adv. Mater.*, 2017, 1703063.
4 B. Russ, A. Glaudell, J. J. Urban, M. L. Chabinyc and R. A. Segalman, *Nat. Rev. Mater.*, 2016, **1**, 16050 EP.
5 K. Walzer, B. Maennig, M. Pfeiffer and K. Leo, *Chem. Rev.*, 2007, **107**, 1233–1271.
6 B. Lüssem, C.-M. Keum, D. Kasemann, B. Naab, Z. Bao and K. Leo, *Chem. Rev.*, 2016, **116**, 13714–13751.
7 I. Salzmann, G. Heimel, S. Duhm, M. Oehzelt, P. Pingel, B. M. George, A. Schnegg, K. Lips, R.-P. Blum, A. Vollmer and N. Koch, *Phys. Rev. Lett.*, 2012, **108**, 035502.
8 H. Méndez, G. Heimel, A. Opitz, K. Sauer, P. Barkowski, M. Oehzelt, J. Soeda, T. Okamoto, J. Takeya, J.-B. Arlin, J.-Y. Balandier, Y. Geerts, N. Koch and I. Salzmann, *Angew. Chem., Int. Ed.*, 2013, **52**, 7751–7755.
9 H. Mendez, G. Heimel, S. Winkler, J. Frisch, A. Opitz, K. Sauer, B. Wegner, M. Oehzelt, C. Rothel, S. Duhm, D. Tobbens, N. Koch and I. Salzmann, *Nat. Commun.*, 2015, **6**, 8560.
10 F. Ghani, A. Opitz, P. Pingel, G. Heimel, I. Salzmann, J. Frisch, D. Neher, A. Tsami, U. Scherf and N. Koch, *J. Polym. Sci., Part B: Polym. Phys.*, 2015, **53**, 58–63.
11 L. Zhu, E.-G. Kim, Y. Yi and J.-L. Brédas, *Chem. Mater.*, 2011, **23**, 5149–5159.
12 J. Gao, J. D. Roehling, Y. Li, H. Guo, A. J. Moulé and J. K. Grey, *J. Mater. Chem. C*, 2013, **1**, 5638–5646.
13 P. Pingel, L. Zhu, K. S. Park, J.-O. Vogel, S. Janietz, E.-G. Kim, J. P. Rabe, J.-L. Brédas and N. Koch, *J. Phys. Chem. Lett.*, 2010, **1**, 2037–2041.
14 D. Di Nuzzo, C. Fontanesi, R. Jones, S. Allard, I. Dumsch, U. Scherf, E. Von Hauff, S. Schumacher and E. Da Como, *Nat. Commun.*, 2015, **6**, 6460.
15 H. Kleemann, C. Schuenemann, A. A. Zakhidov, M. Riede, B. Lüssem and K. Leo, *Org. Electron.*, 2012, **13**, 58–65.
16 I. E. Jacobs, E. W. Aasen, J. L. Oliveira, T. N. Fonseca, J. D. Roehling, J. Li, G. Zhang, M. P. Augustine, M. Mascal and A. J. Moulé, *J. Mater. Chem. C*, 2016, **4**, 3454–3466.
17 I. E. Jacobs, J. Li, S. L. Burg, D. J. Bilsky, B. T. Rotondo, M. P. Augustine, P. Stroeve and A. J. Moulé, *ACS Nano*, 2015, **9**, 1905–1912.
18 D. T. Duong, C. Wang, E. Antono, M. F. Toney and A. Salleo, *Org. Electron.*, 2013, **14**, 1330–1336.
19 D. T. Duong, H. Phan, D. Hanifi, P. S. Jo, T. Nguyen and A. Salleo, *Adv. Mater.*, 2014, **26**, 6069–6073.
20 J. E. Cochran, M. J. N. Junk, A. M. Glaudell, P. L. Miller, J. S. Cowart, M. F. Toney, C. J. Hawker, B. F. Chmelka and M. L. Chabinyc, *Macromolecules*, 2014, **47**, 6836–6846.
21 L. Müller, D. Nanova, T. Glaser, S. Beck, A. Pucci, A. K. Kast, R. R. Schröder, E. Mankel, P. Pingel, D. Neher, W. Kowalsky and R. Lovrincic, *Chem. Mater.*, 2016, **28**, 4432–4439.
22 J. Li, G. Zhang, D. M. Holm, I. E. Jacobs, B. Yin, P. Stroeve, M. Mascal and A. J. Moulé, *Chem. Mater.*, 2015, **27**, 5765–5774.
23 S. Ackling, MSc thesis, University of Adelaide, 2017.
24 P. Pingel and D. Neher, *Phys. Rev. B: Condens. Matter Mater. Phys.*, 2013, **87**, 115209.
25 C. C. Wang, D. T. Duong, K. Vandewal, J. Rivnay and A. Salleo, *Phys. Rev. B: Condens. Matter Mater. Phys.*, 2015, **91**, 085205.
26 M. Meneghetti and C. Pecile, *J. Chem. Phys.*, 1986, **84**, 4149–4162.
27 J. Hynynen, D. Kiefer, L. Yu, R. Kroon, R. Munir, A. Amassian, M. Kemerink and C. Müller, *Macromolecules*, 2017, **50**, 8140–8148.
28 J. Gao, E. T. Niles and J. K. Grey, *J. Phys. Chem. Lett.*, 2013, **4**, 2953–2957.
29 J. Gao, B. W. Stein, A. K. Thomas, J. A. Garcia, J. Yang, M. L. Kirk and J. K. Grey, *J. Phys. Chem. C*, 2015, **119**, 16396–16402.
30 A. R. Chew, R. Ghosh, Z. Shang, F. C. Spano and A. Salleo, *J. Phys. Chem. Lett.*, 2017, **8**, 4974–4980.
31 P. Mori-Sánchez, A. J. Cohen and W. Yang, *Phys. Rev. Lett.*, 2008, **100**, 146401.

32 C. Poelking, M. Tietze, C. Elschner, S. Olthof, D. Hertel, B. Baumeier, F. Würthner, K. Meerholz, K. Leo and D. Andrienko, *Nat. Mater.*, 2014, **14**, 434 EP.
33 N. W. Ashcroft and N. D. Mermin, *Solid State Physics*, Holt, Rinehart and Winston, 1976.
34 J. B. Torrance, *Acc. Chem. Res.*, 1979, **12**, 79–86.
35 J. B. Torrance, J. E. Vazquez, J. J. Mayerle and V. Y. Lee, *Phys. Rev. Lett.*, 1981, **46**, 253–257.
36 M. Avignon, C. A. Balseiro, C. R. Proetto and B. Alascio, *Phys. Rev. B: Condens. Matter Mater. Phys.*, 1986, **33**, 205–209.
37 J. Hubbard and J. B. Torrance, *Phys. Rev. Lett.*, 1981, **47**, 1750–1754.
38 T. F. Harrelson, Y. Q. Cheng, J. Li, I. E. Jacobs, A. J. Ramirez-Cuesta, R. Faller and A. J. Moulé, *Macromolecules*, 2017, **50**, 2424–2435.
39 C. S. Jacobsen and J. B. Torrance, *J. Chem. Phys.*, 1983, **78**, 112–115.
40 Y. Okimoto, S. Horiuchi, E. Saitoh, R. Kumai and Y. Tokura, *Phys. Rev. Lett.*, 2001, **87**, 187401.
41 Z. G. Soos, S. A. Bewick, A. Peri and A. Painelli, *J. Chem. Phys.*, 2004, **120**, 6712–6720.
42 Z. G. Soos and S. Mazumdar, *Phys. Rev. B: Condens. Matter Mater. Phys.*, 1978, **18**, 1991–2003.
43 G. D'Avino, A. Painelli and Z. G. Soos, *Crystals*, 2017, **7**, 144.